Circulation

ORIGINAL RESEARCH ARTICLE

Inhibition of Endothelial Notch Signaling Impairs Fatty Acid Transport and Leads to Metabolic and Vascular Remodeling of the Adult Heart

Editorial, see p 2609

Markus Jabs, PhD
et al

BACKGROUND: Nutrients are transported through endothelial cells before being metabolized in muscle cells. However, little is known about the regulation of endothelial transport processes. Notch signaling is a critical regulator of metabolism and angiogenesis during development. Here, we studied how genetic and pharmacological manipulation of endothelial Notch signaling in adult mice affects endothelial fatty acid transport, cardiac angiogenesis, and heart function.

METHODS: Endothelial-specific Notch inhibition was achieved by conditional genetic inactivation of Rbp-jκ in adult mice to analyze fatty acid metabolism and heart function. Wild-type mice were treated with neutralizing antibodies against the Notch ligand Delta-like 4. Fatty acid transport was studied in cultured endothelial cells and transgenic mice.

RESULTS: Treatment of wild-type mice with Delta-like 4 neutralizing antibodies for 8 weeks impaired fractional shortening and ejection fraction in the majority of mice. Inhibition of Notch signaling specifically in the endothelium of adult mice by genetic ablation of Rbp-jκ caused heart hypertrophy and failure. Impaired heart function was preceded by alterations in fatty acid metabolism and an increase in cardiac blood vessel density. Endothelial Notch signaling controlled the expression of endothelial lipase, Angptl4, CD36, and Fabp4, which are all needed for fatty acid transport across the vessel wall. In endothelial-specific Rbp-jκ–mutant mice, lipase activity and transendothelial transport of long-chain fatty acids to muscle cells were impaired. In turn, lipids accumulated in the plasma and liver. The attenuated supply of cardiomyocytes with long-chain fatty acids was accompanied by higher glucose uptake, increased concentration of glycolysis intermediates, and mTOR-S6K signaling. Treatment with the mTOR inhibitor rapamycin or displacing glucose as cardiac substrate by feeding a ketogenic diet prolonged the survival of endothelial-specific Rbp-jκ–deficient mice.

CONCLUSIONS: This study identifies Notch signaling as a novel regulator of fatty acid transport across the endothelium and as an essential repressor of angiogenesis in the adult heart. The data imply that the endothelium controls cardiomyocyte metabolism and function.

The full author list is available on page 2606

Key Words: angiogenesis ■ animal model cardiovascular disease ■ endothelial cell ■ metabolism

Sources of Funding, see page 2606

http://circ.ahajournals.org

Clinical Perspective

What Is New?

- This study shows that Notch signaling in the endothelium controls blood vessel formation and fatty acid transport in the adult mouse heart.
- Inhibition of Notch signaling in the vasculature leads to expansion of the cardiac vasculature and impairment of fatty acid transport to cardiomyocytes.
- This results in metabolic reprogramming and heart failure.

What Are the Clinical Implications?

- Notch signaling is a promising target in oncology.
- Pharmacological inhibition of Notch signaling could lead to heart failure because of vascular and metabolic remodeling of the heart.

Endothelial cells (ECs) form tubes for the transport of blood; in addition, ECs regulate organogenesis, tissue regeneration, stem cell differentiation, or tumor progression in a paracrine (angiocrine) fashion.[1,2] Given that ECs are in close proximity to almost every other cell type, they are ideally suited to control homeostasis. Although this may also be important for controlling the distribution of nutrients to parenchymal cells, little is known about this process.

Located at the interface between plasma and parenchymal cells, EC heterogeneity provides organ-specific vascular beds.[1] For instance, sinusoidal liver ECs form gaps and do not provide a physical barrier for nutrient transport, whereas the continuous endothelium in muscle, heart, lung, or brain requires transcellular transport of nutrients. EC fatty acid transport is facilitated by PPARγ and Meox2/Tcf15,[3,4] and previous studies have discussed how vascular endothelial growth factor B secreted from cardiomyocytes stimulates EC fatty acid transport.[5–7]

The activity of Notch signaling in various cell types is influenced by plasma glucose[8–11] and inflammatory lipids,[12] suggesting a link between the metabolic status and Notch signaling activity. Notch signaling is an intercellular communication system. The binding of ligands (Delta-like [DLL] and Jagged) triggers the cleavage of Notch receptors to release the intracellular domain (Notch-ICD) that enters the nucleus and interacts with Mastermind-like–1 and the Rbp-jκ complex to act as a transcription factor. In the developing vasculature and in solid tumors, DLL4/Notch signaling restrains angiogenesis,[13] whereas in the adult quiescent endothelium, the role of Notch signaling is not yet understood.

Notch signaling is an interesting target for therapeutic interventions in oncology. However, severe congestive heart failure occurred in a substantial proportion of patients treated with different DLL4-blocking antibodies in phase I studies[14,15] that target Notch signaling predominantly in ECs and a few other cell types. The reason for this outcome remains elusive.

METHODS

The authors declare that all supporting data are available within the article and its online supplementary files.

Please refer to the Expanded Methods in the online-only Data Supplement for experimental details.

Animal Studies

The study was approved by Institutional and Regional Animal Research Committees. All animal procedures were in accordance with institutional guidelines and performed according to the guidelines of the local institution and local government (Regierungspräsidium Karlsruhe).

Rbpj$^{i\Delta EC}$ mice (Cdh5-CreERT2,Rbpj$^{lox/lox}$) were obtained by crossing Cdh5-CreERT2 mice with *Rbpj*$^{lox/lox}$ mice[16] and injected with 1.5 mg tamoxifen IP for 5 consecutive days. Triacylglycerols, total ketone bodies, and nonesterified fatty acids were measured using kits from Sigma and Wako Diagnostics. Glucose-6-phosphate was determined with a kit from Cayman Chemical Company. Acyl-CoAs were extracted from tissues and measured as described.[17,18] Mice were not anesthetized during transthoracic echocardiography.[19] Long-chain fatty acid organ uptake was assessed as described.[20] DLL4-blocking antibodies were from Genentech.[21]

Statistical Analysis

The results are presented as mean and SEM. SigmaPlot 12.5 (Systat Software) was used for statistical analysis. Unpaired 2-tailed Student's *t* test was used for comparisons of 2 groups (most of the presented experiments). Significance between >2 groups was tested by 2-way analysis of variance using the Holm-Sidak method as a post hoc test. The log-rank test was used to compare survival of mouse cohorts. $P<0.05$ was considered statistically significant.

RESULTS

Neutralizing DLL4 Antibodies Impairs Heart Function in Mice

Notch1 is expressed in variable amounts in ECs and several other cell types.[22] We observed Notch1 expression in ECs of heart, skeletal muscle, liver, and white adipose tissue of adult mice (Figure 1A). In the hearts of wild-type mice, there was in particular Notch1 activity in blood vessels as demonstrated by the presence of Notch1-ICD (Figure 1B). Pharmacological targeting of Notch signaling specifically in ECs is not possible to date. However, the expression of the Notch ligand DLL4 is more restricted to the vasculature, making this an attractive target to inhibit vascular Notch signaling. Inspired by the fact that heart failure was observed in phase I trials using neutralizing DLL4 antibodies,[14,15] we aimed to test whether neutralizing antibodies against murine DLL4[23]

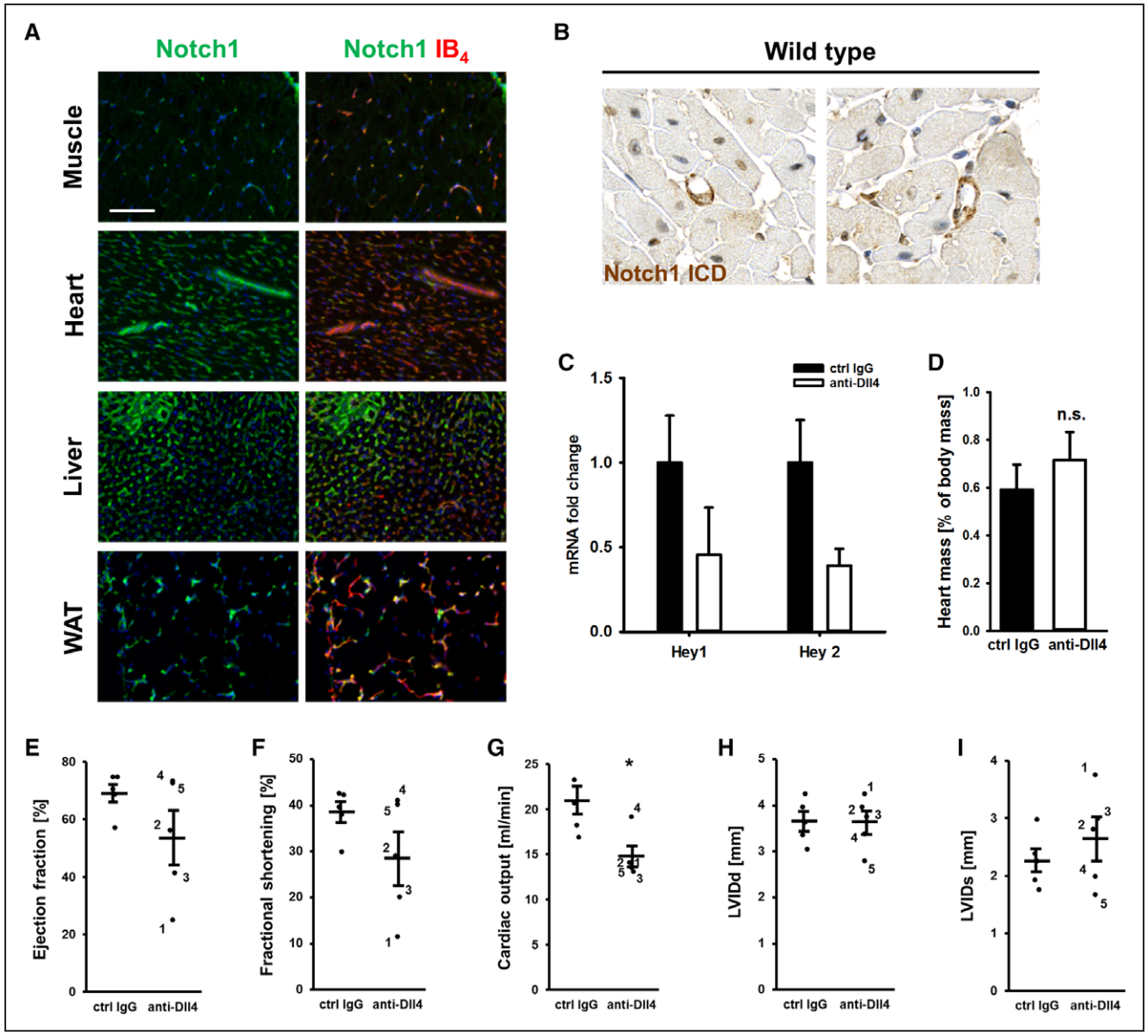

Figure 1. Notch1 expression in the vasculature and cardiac effects of DLL4 blocking antibodies.
A, Sections of gastrocnemius muscle, heart, liver, and perigonadal white adipose tissue (WAT) from adult C57BL/6 mice stained against Notch1 (green). Endothelial cells were stained with TRITC-IB_4-lectin (*Griffonia simplicifolia*) (red), and nuclei were stained with DAPI (blue). Scale bar, 100 µm. **B,** Antibody staining against activated Notch1 (Notch1-ICD; brown) in left ventricular wall of adult C57BL/6 mice counterstained with hematoxylin. Representative images shown. Scale bar, 100 µm. **C** through **I,** Adult C57BL/6 mice were treated with DLL4 neutralizing antibodies and control antibodies for 8 weeks. **C,** mRNA expression levels of the Notch target genes *Hey1* and *Hey2* in freshly isolated lung endothelial cells. **D,** Heart weight in relation to body mass. **E** through **I,** Transthoracic echocardiography of 5 control-treated mice and 5 mice (labeled 1–5) treated with DLL4 antibodies. DLL4 indicates Delta-like ligand 4; ICD, intracellular domain; LVID, left ventricle inner diameter during systole and diastole; and n.s., not significant. Mean and SEM shown. **P*<0.05.

would also impair heart function in C57BL6 wild-type mice. Eight weeks after the first injection, freshly isolated ECs had lower mRNA expression levels of *Hey1* and *Hey2*, which is indicative of decreased Notch signaling activity (Figure 1C). The mice had no changes in body weight compared with controls as observed before,[23] and the heart–to–body-weight ratio was slightly but not significantly increased (Figure 1D). Transthoracic echocardiography revealed that anti-DLL4 treatment led to a reduction in ejection fraction and fractional shortening in 3 of 5 mice (Figure 1E through 1I).

EC-Specific Rbp-jκ Ablation Impairs Heart Function

To test whether the inhibition of Notch signaling selectively in the endothelium contributes to the development of heart failure, we inactivated the *Rbpj* gene–encoding

Rbp-jκ, the essential transducer downstream of all 4 Notch receptors, specifically in ECs.[16] Tamoxifen-driven genetic deletion of *Rbpj* in adult *Cdh5-CreERT2*,*Rbpj*$^{lox/lox}$ mice (*Rbpj*$^{i\Delta EC}$ mice) resulted in robust reduction of Rbp-jκ protein specifically in ECs but not in whole-tissue lysates representing multiple cell types (Figure IA and IB in the online-only Data Supplement). Cre-negative tamoxifen-treated littermates were used as controls. In addition, the cardiac phenotype was also analyzed in Cre-positive tamoxifen-treated mice lacking the floxed allele. As reported before,[23] both controls showed no significant differences.

Heart morphology and weight as well as cardiac pump function were not altered 4 to 5 weeks after injection of tamoxifen (post injection [p.i.]) that leads to endothelial *Rbpj* gene ablation (Figure IC through IK in the online-only Data Supplement). At 6 to 7 weeks p.i., there was a decrease in ejection fraction (27% versus 63%, P=0.022). Surface electrocardiogram showed no obvious alterations compared with control mice (Figure IL in the online-only Data Supplement). At 8 to 10 weeks p.i., the mice died.

Histopathologic examination of hearts from *Rbpj*$^{i\Delta EC}$ mice 8 weeks p.i. revealed marked hypertrophy of cardiomyocytes, which exhibited larger variance in nuclear size and more cytoplasm, as well as thickening of the left ventricular wall and septum (Figure 2A and 2B and Figure IIA in the online-only Data Supplement). There were no signs of fibrosis (Figure IIB in the online-only Data Supplement), hyperplasia, necrosis, or apoptosis. Electron microscopy showed normal arrangement of the cardiac muscle fibers, intercalated discs, and normal morphology and localization of mitochondria. However, the mitochondrial size was increased and the mitochondria often contained electron-dense particles likely representing calcium precipitates (Figure 2C and Figure IIC and IID in the online-only Data Supplement), which can form because of high cytoplasmic calcium levels.[24] Cardiac calcium handling can be impaired because of diminished ATP,[25] and indeed there was a significant reduction of ATP levels in heart lysates of *Rbpj*$^{i\Delta EC}$ mice (Figure 2D). The heart–to–body-weight ratio was >70% higher in *Rbpj*$^{i\Delta EC}$ than in control animals (Figure 2E). Echocardiography revealed that the left ventricle was massively enlarged and had an ejection fraction of <20% (Figure 2F through 2I, Figure IIE through IIH in the online-only Data Supplement, and Movie in the online-only Data Supplement). The lungs of *Rbpj*$^{i\Delta EC}$ mice were significantly heavier than controls (Figure 2E), indicating pulmonary edema because of reduced pumping function of the left ventricle. This finding was accompanied by an increased expression of the natriuretic peptide *Bnp* (Figure 2J).

Heart failure often leads to a switch in gene expression from the adult toward the fetal gene expression program. The fetal heart has a strong preference to carbohydrates over fatty acids as substrates for energy provision and shows lower expression of genes associated with fatty acid oxidation.[26] We detected clear evidence for induction of the fetal gene expression program in the hearts of *Rbpj*$^{i\Delta EC}$ mice 8 weeks p.i. with altered expression of glucose transporter-4 (Glut4), pyruvate dehydrogenase kinase isoform-2 (Pdk2), acyl-CoA dehydrogenase, long chain and medium chain (Acadl, Acadm), citrate synthase (Cs), carnitine palmitoyltransferase-1b (Cpt1b), collagen type IIIα (Col3a), and myosin heavy polypeptide-6 (Myh6) (Figure 2J).

EC-Specific Rbp-jκ Ablation Leads to Increased Cardiac Blood Vessel Density

EC Notch signaling restrains angiogenesis during development, ischemia, tissue repair, and tumor growth.[13] To test whether Notch inhibition would also lead to increased blood vessel growth during heart hypertrophy and failure, blood vessel density was determined. There was already a pronounced alteration in cardiac blood vessel morphology in several spots throughout both ventricles of *Rbpj*$^{i\Delta EC}$ mice at 4 weeks p.i., and the CD31-positive area was increased compared with controls (Figure 3A and 3B). Even in the hypertrophic hearts 7 weeks p.i., there was still a substantial increase in the CD31-positive area. In skeletal muscle, vessel density was increased at 8 weeks p.i., whereas in the brain, no such changes were observed (Figure 3A, 3C, and 3D). The increased cardiac vessel density was associated with higher *CD31* and *Vegfr2* mRNA levels in heart lysates, whereas *Vegf-a* levels, indicative of hypoxia, were not increased (Figure 3E).

To test whether these vascular alterations would severely alter blood perfusion, we first analyzed skin perfusion and detected no significant changes (Figure 3F). Second, Hoechst dye 33342 was injected intravenously, and mice were euthanized 60 seconds later. The dye reached essentially all cell nuclei of cardiac muscle in *Rbpj*$^{i\Delta EC}$ (8 weeks p.i.) and control mice, indicating no major defect in blood perfusion (Figure 3G). The same was observed in skeletal muscle (data not shown).

Elevated Plasma Triacylglycerols and Nonesterified Fatty Acid Levels in *Rbpj*$^{i\Delta EC}$ Mice

Because the observed vascular alterations appeared unlikely as the sole cause of heart failure, we searched for additional means by which altered EC function could contribute to the deterioration of heart function. Changes in cardiac metabolism might cause heart failure.[27] ECs play an important role in shuttling fatty acids to subendothelial cells[3,4] and could thereby lead to metabolic remodeling in case nutrient transport is impaired.

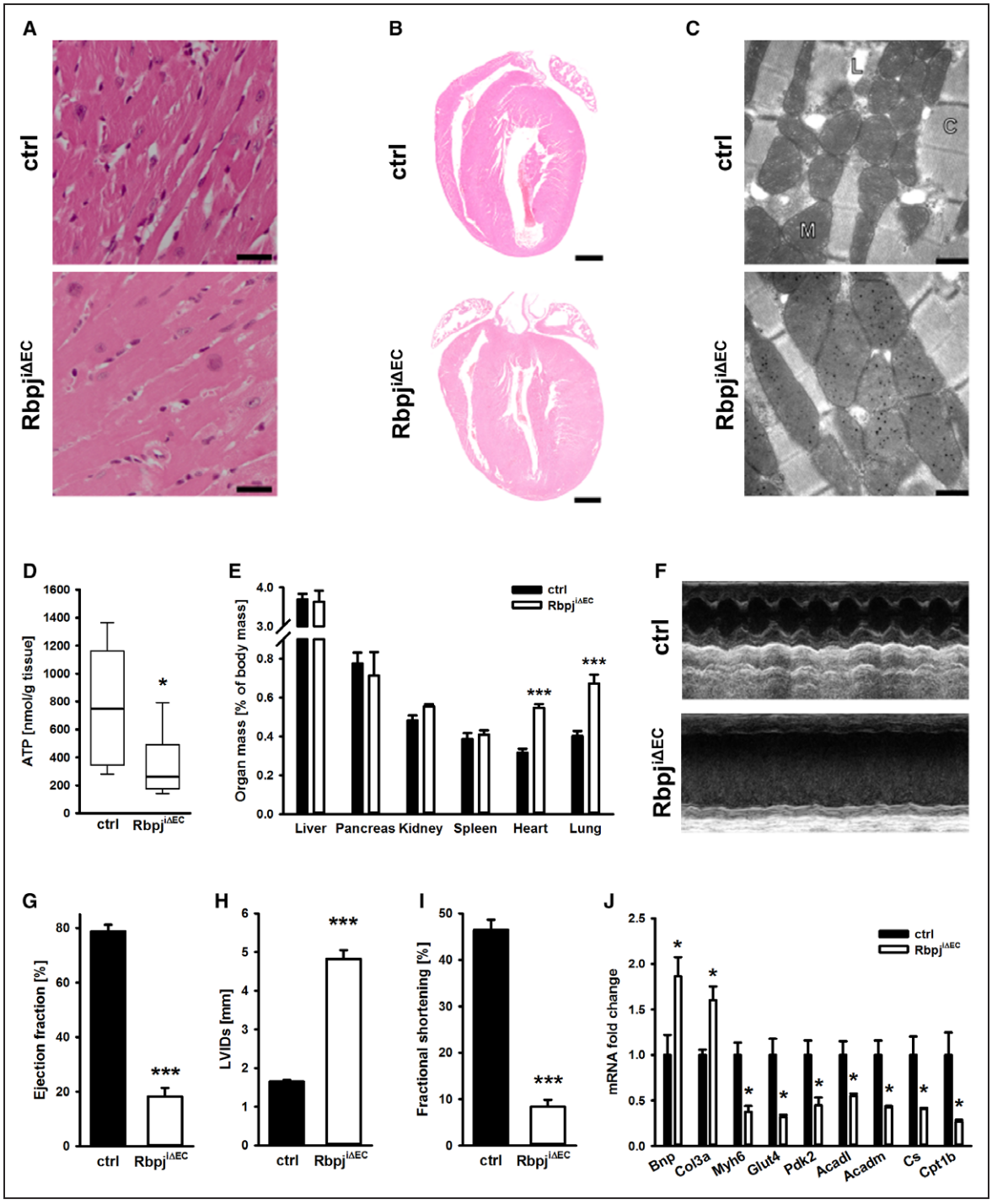

Figure 2. Endothelial-specific *Rbpj* inactivation causes cardiac hypertrophy and heart failure.
A and **B,** H&E staining of hearts shows cardiac hypertrophy 7 weeks after *Rbpj* gene recombination. Scale bar, 25 µm (**A**), 1 mm (**B**). **C,** Electron micrographs of hearts 8 weeks after gene recombination (L, lipid droplet; C, cardiac muscle; M, mitochondrion). Scale bar, 500 nm. **D,** ATP in heart lysates 8 weeks after gene inactivation (n=10 control and 11 $Rbpj^{i\Delta EC}$ mice). **E,** Relative organ mass 8 weeks after *Rbpj* recombination (n=4 control and n=5 $Rbpj^{i\Delta EC}$ mice). **F** through **I,** Eight weeks after gene recombination, transthoracic echocardiography shows impaired heart function in $Rbpj^{i\Delta EC}$ mice (n=5 mice). **J,** Transcript levels of the cardiac hypertrophy and heart failure marker *Bnp* (natriuretic peptide type B) and markers of the fetal cardiac gene expression program in heart lysates (*Col3a1*, type III collagen; *Myh6*, alpha myosin heavy chain; *Glut4*, glucose transporter-4; *Pdk2*, pyruvate dehydrogenase kinase isozyme-2; *Acadl*, acyl-coenzyme-A dehydrogenase long-chain; *Acadm*, acyl-coenzyme A dehydrogenase medium chain; *Cs*, citrate synthase; *Cpt1b*, carnitine palmitoyltransferase-1b muscle; n=4). H&E indicates hematoxylin and eosin; and LVIDs, left ventricle inner diameter during systole. Mean and SEM or representative pictures shown. Box plot depicts median and percentiles (10th, 25th, 75th, 90th). **P*<0.05; ****P*<0.001.

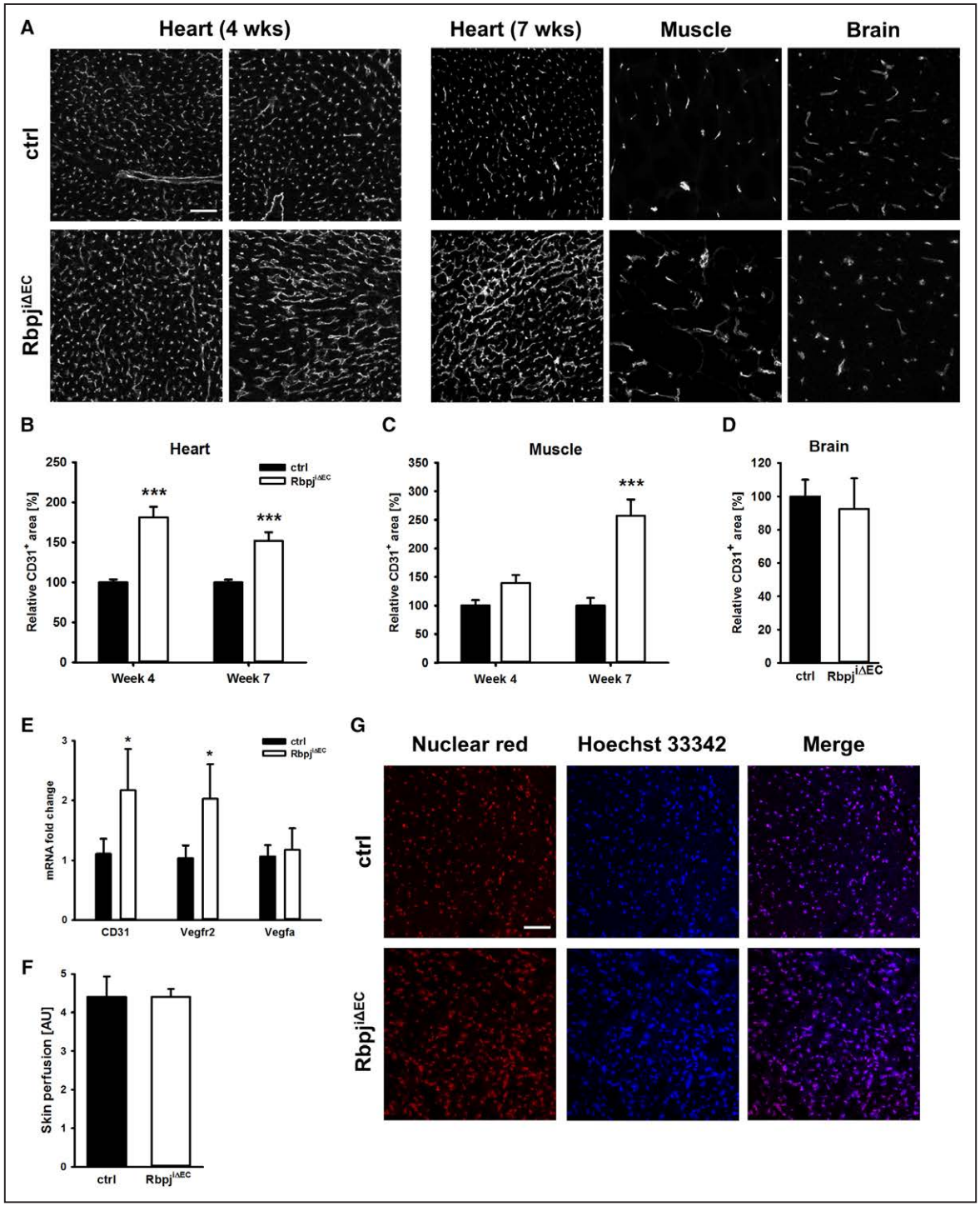

Figure 3. Endothelial-specific Rbpj inactivation increases cardiac vessel density.

A, Staining sections of heart (left ventricular wall), gastrocnemius muscle, and brain against the endothelial marker CD31 at 4 and 7 or 8 weeks after gene recombination. Four weeks after endothelial *Rbpj* gene recombination, there were areas of normal vascular morphology and some with increased vessel size and vessel density (representative pictures shown). **B** through **D,** Quantification of the CD31-positive to total area in heart, muscle, and brain 4 (n=3 mice) and 7 weeks (n=5 mice) after gene recombination. **E,** mRNA expression of *CD31*, *Vegfr2* (vascular endothelial growth factor receptor 2), and *Vegf-a* (vascular endothelial growth factor A) in heart lysates of *Rbpj*$^{i\Delta EC}$ and control mice 7 weeks after gene recombination (n=4 mice). **F,** Blood perfusion in the ear skin determined by laser-Doppler analysis 7 weeks after gene recombination (n=6 control and 7 *Rbpj*$^{i\Delta EC}$ mice). **G,** Hoechst dye 33342 (blue) was injected into a tail vein 7 weeks after gene recombination (n=5 mice), and mice were euthanized 60 seconds later. Fixed heart sections were counterstained with nuclear red to identify cell nuclei, to which the dye was transported (representative images). Scale bars, 50 µm. Mean and SEM shown. *P<0.05; ***P<0.001.

Because the activity of Notch signaling is influenced by several metabolites,[8–12] we aimed to analyze whether EC Notch signaling could be involved in controlling the metabolite flux from plasma to muscle cells.

Rbpj$^{i\Delta EC}$ mice showed no differences in body fat and lean masses compared with Cre-negative littermate controls 8 weeks p.i. (Figure II I in the online-only Data Supplement). The morphology of Langerhans islets (Figure 4A) and storage of carbohydrates in the liver were comparable to controls (data not shown). However, the plasma of *Rbpj*$^{i\Delta EC}$ mice showed elevated levels of triacylglycerols and nonesterified fatty acids (Figure 4B and 4C), and mice developed fatty liver (Figure 4D). This outcome could already be observed at 3 to 4 weeks p.i., when cardiac output function was still normal. This finding indicated that EC Notch signaling might be needed for the transendothelial transport of fatty acids.

EC Notch Signaling Is Needed for Clearance of Plasma Triacylglycerols

Triacylglycerols are processed into fatty acids by lipases apically bound to ECs. It is important to note that the discontinuous liver endothelium is no barrier for fatty acid uptake by hepatocytes. In turn, the continuous endothelium in muscle provides transcellular transport of fatty acids.[1]

First, we analyzed potential crosstalk between endothelium and fatty acid metabolism in liver. Liver histology showed regular trabecular architecture. Fibrosis, necrosis, or overt inflammation were not present (Figure 4A). The expression of genes involved in lipogenesis in liver lysates of *Rbpj*$^{i\Delta EC}$ mice did not indicate increased hepatic triacylglycerol production, and the expression of β-oxidation enzymes was not altered (Figure 4E and 4F). Furthermore, the blockade of vascular lipolysis by tyloxapol showed that hepatic triacylglycerol production was not increased in *Rbpj*$^{i\Delta EC}$ mice compared with controls (Figure 4G). Because hepatic lipid metabolism unlikely explained the accumulation of triacylglycerol in the liver and plasma, we hypothesized that transendothelial fatty acid transport in organs containing a continuous endothelium could be impaired.

To test this theory, we first challenged *Rbpj*$^{i\Delta EC}$ mice (4 to 5 weeks p.i.) with an oral application of olive oil. As expected, plasma triacylglycerol levels first increased to a maximum, which was similar in both genotypes. Then the circulatory triacylglycerol levels of *Rbpj*$^{i\Delta EC}$ mice decreased more slowly than those of controls, suggesting lower triacylglycerol clearance into the tissues as indicated by a smaller slope between peak and end of the experiment (Figure 4H and 4I). It is important to note that the fat resorption from the gut did not seem to be impaired because the defecation rate and the triacylglycerol concentration in feces were similar in both genotypes (Figure 4J and 4K).

EC Notch Signaling Is Required for Vascular Lipolysis and Transport of Nonesterified Fatty Acids

The triacylglycerol clearance test indicated that loss of EC Notch signaling leads to either decreased lipase activity or reduced EC transcytosis of fatty acids. Indeed, we detected a ≈50% reduction of plasma lipase activity in *Rbpj*$^{i\Delta EC}$ mice (Figure 5A). Second, we analyzed whether lipase activity and the transendothelial fatty acid transport would be controlled by Notch signaling. To this end, the uptake of intravenously injected tracer^{3}H-R-bromopalmitate, a slowly metabolized palmitate analogue, into different organs was measured. Compared with controls, *Rbpj*$^{i\Delta EC}$ mice (5 weeks p.i.) had lower uptake rates of palmitate into heart and skeletal muscle. As expected, no alterations were seen in the liver (Figure 5B and 5C), in which the sinusoidal endothelium does not act as a tight barrier.

Based on these experiments, we expected to detect diminished levels of activated fatty acids (acyl-CoA) in cardiac and skeletal muscle of *Rbpj*$^{i\Delta EC}$ mice. Indeed, acyl-CoA levels were reduced to 80% in skeletal muscle and to 55% in the hearts of *Rbpj*$^{i\Delta EC}$ mice compared with controls (Figure 5D). Detailed analysis of fatty acids bound to carnitine revealed a decrease in long-chain but not in medium- or short-chain fatty acids in cardiac muscle (Figure 5E).

Notch Signaling Facilitates Uptake of Fatty Acids Into Cultured ECs

Next, we aimed to analyze the transport of fatty acids into ECs in an in vitro setting to exclude the potential effects of unknown factors that may interfere with such transport in transgenic mouse models. We first tested whether Notch signaling generally alters paracellular flux through an EC monolayer in vitro because this would affect monitoring the specific transport of fatty acids. Therefore, we manipulated Notch signaling activity in primary human umbilical venous ECs (HUVECs), the prototypic tool for EC research.

Notch inhibition increased paracellular permeability as determined by measuring the transendothelial electric resistance and capacity (Figure IIIA in the online-only Data Supplement). In addition, the flux of fluorescent 4-kDa dextran tracers in a transwell filter assay was increased after Notch inhibition, whereas no such changes were observed with 40-kDa dextran tracers (Figure IIIB and IIIC in the online-only Data Supplement), indicating a size-selective opening of paracellular transport routes.

In vivo, extravasation of Evans blue (bound to plasma proteins) was, however, not increased in *Rbpj*$^{i\Delta EC}$ mice compared with littermate controls under basal conditions or after stimulation with histamine. In the latter case, there was even a slight reduction of paracellular permeability compared with control animals (Figure IIID in the online-only Data Supplement). Likewise in a

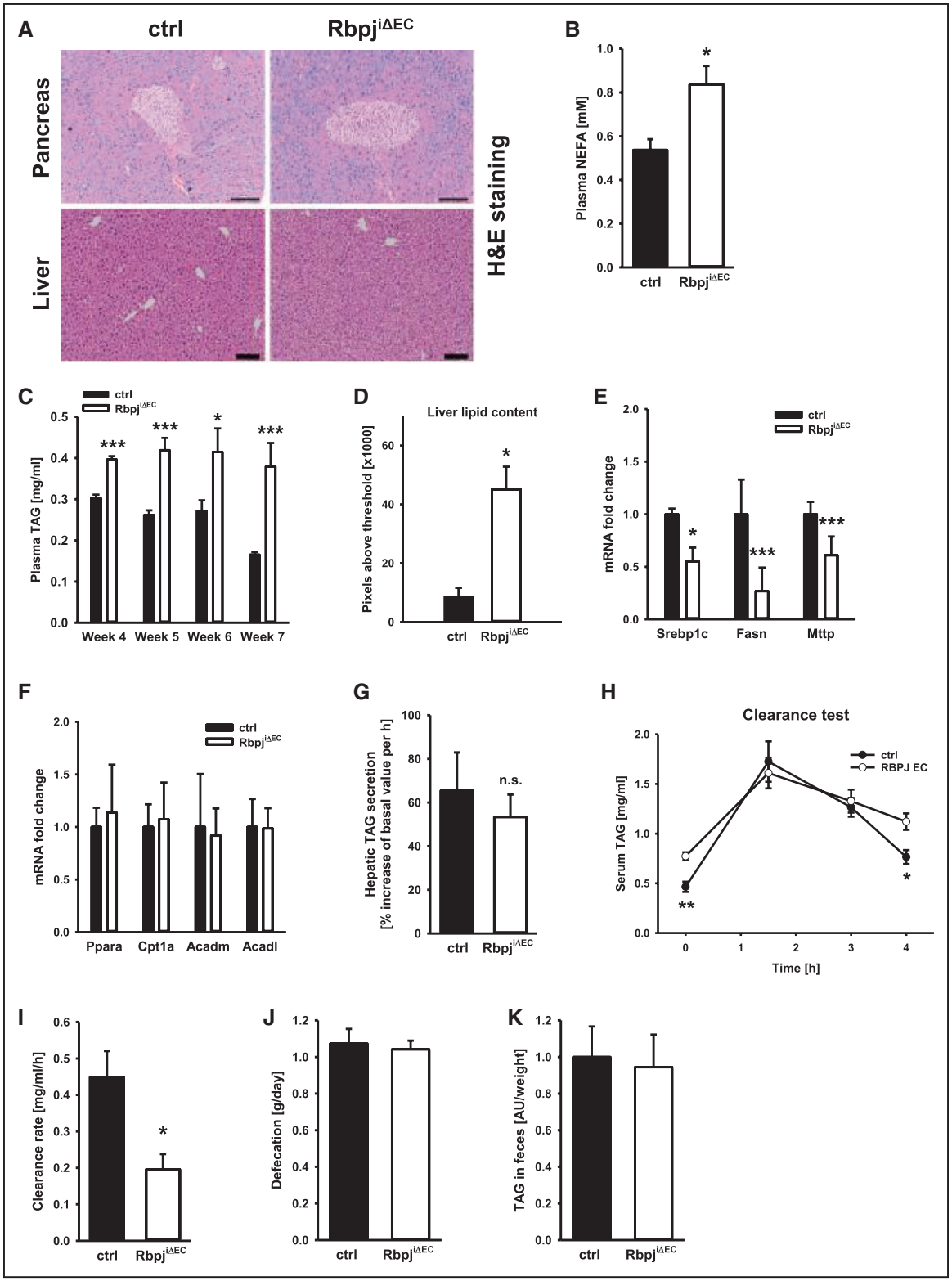

Figure 4. Endothelial Notch signaling regulates systemic lipid clearance.
A, H&E (hematoxylin and eosin) staining of pancreatic islets and liver. **B** and **C,** Nonesterified fatty acids (NEFAs) and plasma triacylglyceride (TAG) concentration 6 weeks after endothelial *Rbpj* gene inactivation (n=5 mice). **D,** Liver lipid content quantified by determination of Oil Red O–stained droplets (n=3 mice). **E** and **F,** Hepatic expression of key genes involved in lipogenesis and lipolysis (n≥3 mice). **G,** Hepatic TAG secretion of *Rbpj*$^{i\Delta EC}$ mice and controls (n=6 mice). **H** through **K,** At 4 to 5 weeks after gene recombination, fat clearance test with oral gavage of olive oil (n=6 control and 7 *Rbpj*$^{i\Delta EC}$ mice) shows impaired TAG clearance in *Rbpj*$^{i\Delta EC}$ mice after serum TAG levels reached their highest level. Clearance rate was calculated as the slope from maximum to end. Defecation and TAG content of feces (n=4). Mean and SEM or representative pictures shown. Scale bar, 100 µm. **P*<0.05; ***P*<0.01; ****P*<0.001.

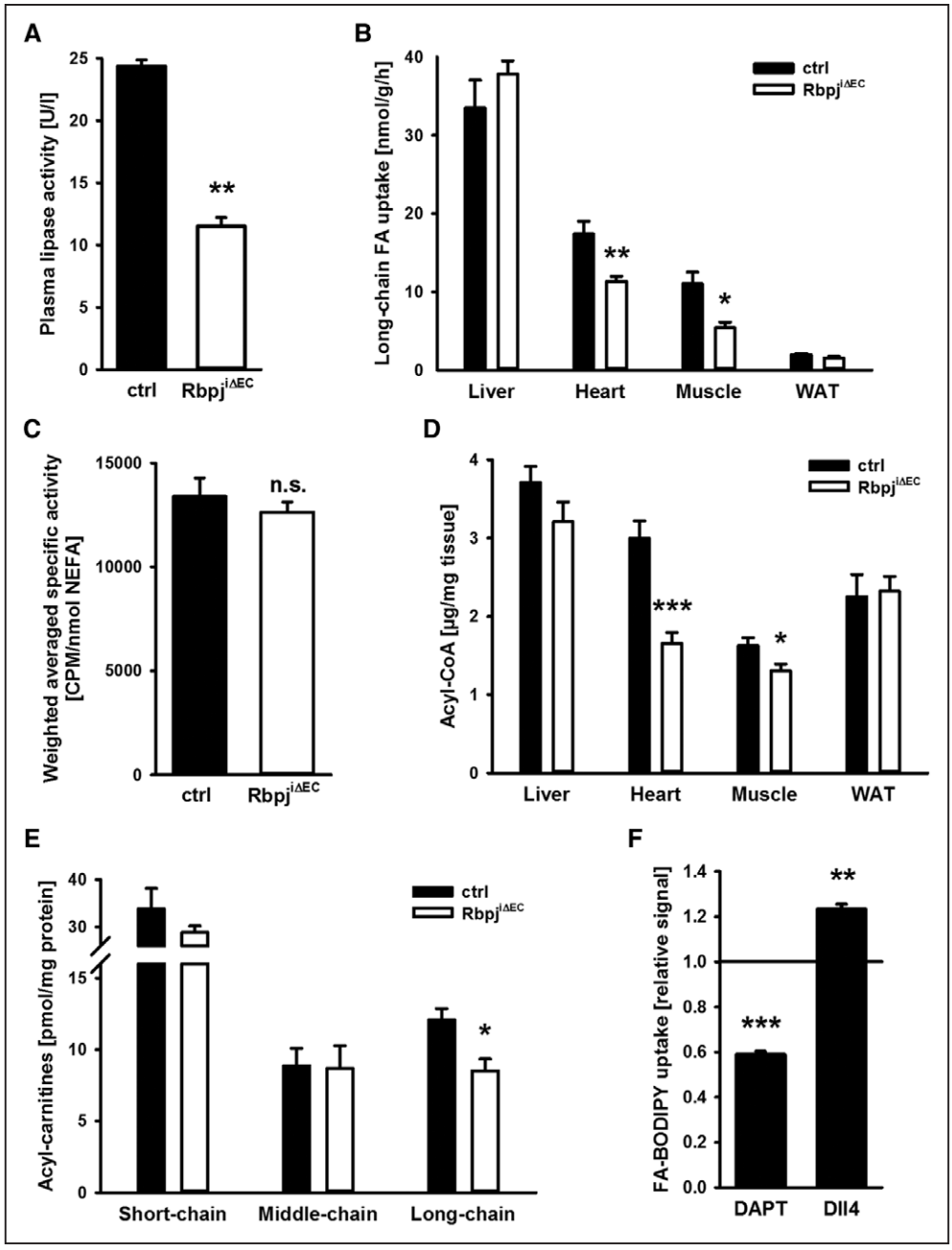

Figure 5. EC-specific *Rbpj* ablation disturbs fatty acid transport.
A, Plasma lipase activity after heparin injection was diminished in *Rbpj*$^{i\Delta EC}$ mice (n=3). **B** and **C,** Uptake of the long-chain fatty acid (FA) analogue ^{3}H-R-bromopalmitate into muscle tissue but not liver and white adipose tissue (WAT) was impaired in *Rbpj*$^{i\Delta EC}$ mice 5 weeks after gene recombination. Weighted averaged activity of the ^{3}H-R-bromopalmitate tracer during the uptake experiment (n=6 mice). **D** and **E,** Concentration of acyl-CoA in several tissues (n=10 control and 7 *Rbpj*$^{i\Delta EC}$ mice) and of acyl-carnitines with different chain length in heart (n=5 control and 4 *Rbpj*$^{i\Delta EC}$ mice). **F,** Uptake of fluorescently labeled palmitic acid (FA-BODIPY) into primary human venous EC (HUVEC) on Notch signaling inhibition (DAPT) or activation (DLL4 coating) (n=3). Mean and SEM shown. *P<0.05; **P<0.01; ***P<0.001.

peritonitis assay, *Rbpj*$^{i\Delta EC}$ mice exhibited no signs of increased permeability compared with controls (Figure IIIE and IIIF in the online-only Data Supplement). Basal paracellular permeability of 10- and 40-kDa tracers was similar in the hearts of *Rbpj*$^{i\Delta EC}$ mice compared with controls (Figure IIIG and IIIH in the online-only Data Supplement).

Hence, the inhibition of Notch signaling promotes paracellular flux of small molecules in vitro but not in vivo. For this reason, we could not determine how Notch inhibition alters the transport of fatty acids through an EC monolayer in vitro. However, we could detect that the inhibition of Notch signaling impaired the uptake of

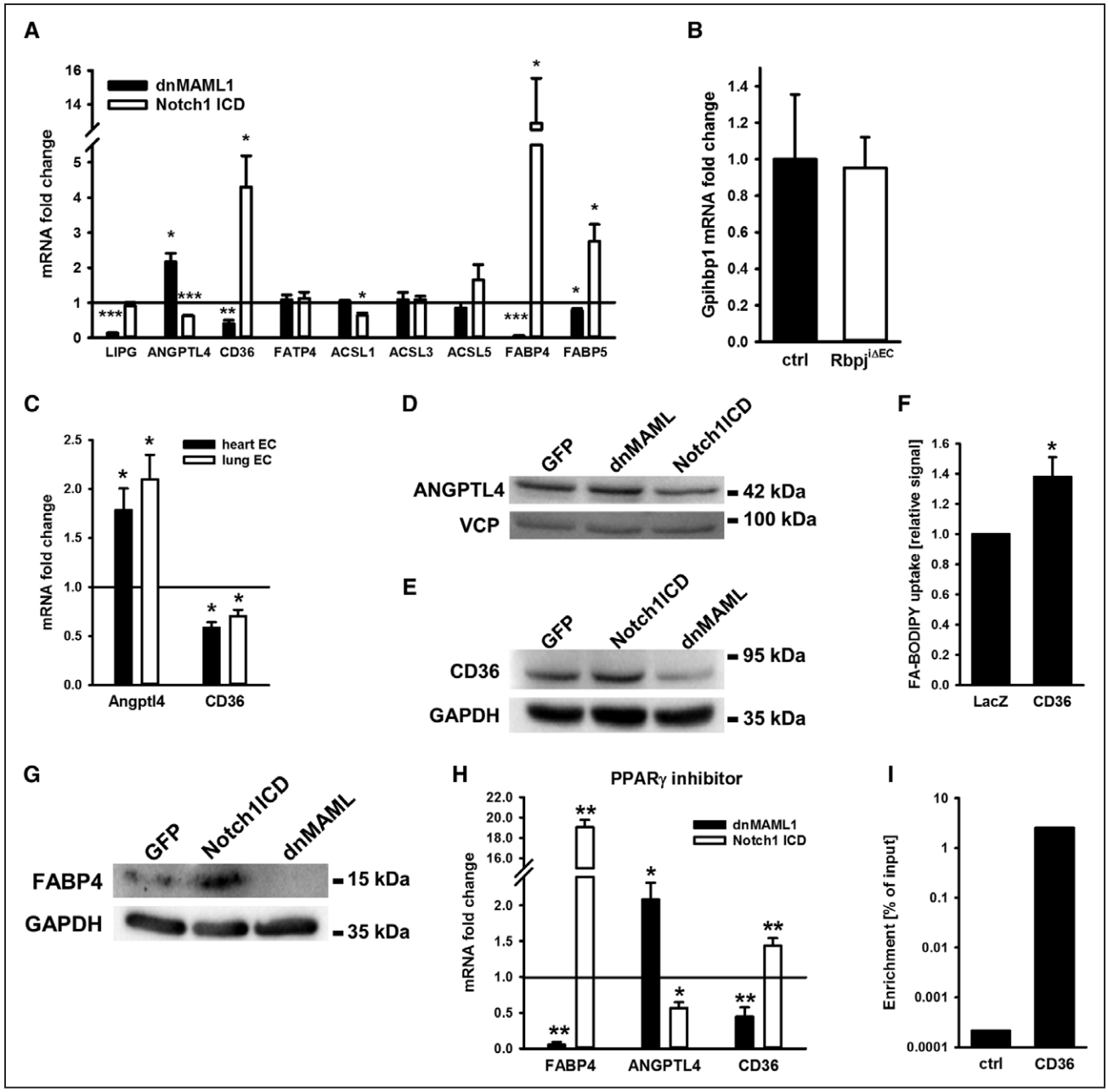

Figure 6. Notch signaling controls transcription of genes involved in endothelial TAG hydrolysis and transport of fatty acids.

A, Expression of genes involved in uptake and transendothelial shuttling of fatty acids in HUVEC on genetic Notch manipulation (*LIPG*, lipase G, endothelial type; *ANGPTL4*, angiopoietin like 4; *FATP4*, solute carrier family 27 member 4; *ACSL*, acyl-CoA synthetase long-chain family member; and *FABP*, fatty acid binding protein) (n=3). **B,** Expression of *Gpihbp1* (glycosylphosphatidylinositol anchored high density lipoprotein binding protein-1) in primary heart ECs isolated from controls and *Rbpj*$^{i\Delta EC}$ mice (n=4). **C,** Expression of *Angptl4* and *CD36* mRNA in freshly isolated lung and heart ECs (n=3 control and 4 *Rbpj*$^{i\Delta EC}$ mice). **D** and **E,** Western blotting to determine the expression of Angptl4 and CD36 protein in primary murine heart endothelial cells overexpressing GFP, dnMAML (dominant-negative Mastermind-like-1) to block Notch activity, or Notch1-ICD (intracellular domain). **F,** Uptake of fluorescently labeled palmitic acid (FA-BODIPY) into HUVEC on forced CD36 expression (n=4). **G,** Expression of FABP4 protein in primary murine heart endothelial cells overexpressing GFP, Notch1-ICD, or dnMAML. **H,** Expression of *FABP4*, *ANGPTL4*, and *CD36* mRNA on Notch manipulation in the presence of 1 μM T0070907 (PPARγ inhibitor) in HUVEC (n=3). **I,** Enrichment of DNA from a putative Rbpj-binding motif in the CD36 promoter of HUVEC after precipitation with an antibody recognizing Rbpj (representative experiment). Results are shown as mean and SEM or representative pictures. **P*<0.05; ***P*<0.01; ****P*<0.001.

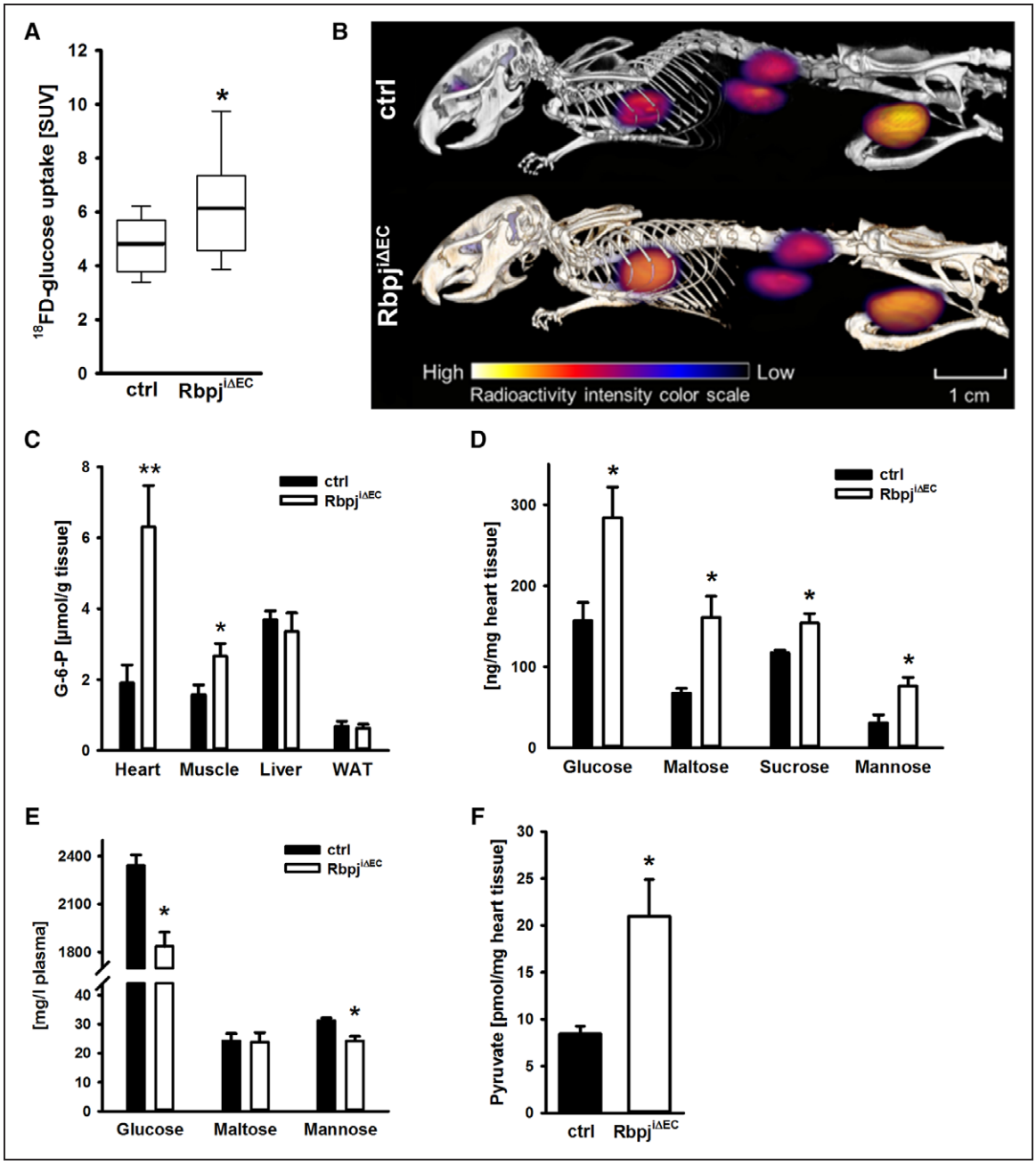

Figure 7. Elevated glucose uptake and metabolism in *Rbpj*$^{i\Delta EC}$ hearts.
A and **B,** Uptake of ^{18}F-fluoro-2-deoxy-D-glucose into hearts (n=10 mice). **C,** Glucose-6-phosphate (G-6-P) in heart, gastrocnemius muscle, liver, and perigonadal white adipose tissue (WAT) of control and *Rbpj*$^{i\Delta EC}$ mice (n=7). **D** through **F,** Concentration of several carbohydrates and pyruvate in hearts (n=5) or plasma (n=7 control and 3 *Rbpj*$^{i\Delta EC}$ mice). SUV indicates standardized uptake value. Mean and SEM. Box plot depicts median and percentiles (10th, 25th, 75th, 90th). *P<0.05; **P<0.01.

a fluorescent palmitate analogue into HUVEC, whereas this was increased on Notch stimulation by recombinant DLL4 (Figure 5F).

Notch Controls Expression of *LIPG* and *ANGPTL4* to Facilitate Vascular Lipolysis

Next, we aimed to identify mechanisms for how EC Notch signaling controls fatty acids transport. Notch/Rbp-jκ signaling activates gene expression by binding to promoter elements or represses gene expression indirectly by the induction of HES and HEY transcriptional repressors. The activity of Notch signaling was inhibited by the expression of dominant-negative Mastermind-like–1 (dnMAML) and enhanced by the expression of Notch1-ICD in HUVEC, and efficiency was controlled by *quantitative polymerase chain reaction* assessing target genes (*HEY1*, *HEY2*, *DLL4*,

EFNB2). Notch inhibition led to decreased transcription of endothelial lipase (*LIPG*) (Figure 6A), which hydrolyzes mainly phospholipids but also triacylglycerol.

In addition to hydrolysis by LIPG, fatty acids can also be released from triacylglycerol-containing lipoproteins by lipoprotein lipase. This lipase is synthesized and secreted by parenchymal cells (eg, cardiomyocytes) and subsequently bound at the apical EC surface by Gpihbp1.[28,29] The expression of *Gpihbp1* in primary cardiac ECs isolated from *Rbpj*$^{i\Delta EC}$ mice was similar to expression in cells isolated from controls (Figure 6B).

Vascular lipolysis is also controlled by the noncompetitive lipoprotein lipase inhibitor angiopoietin-like 4 (*ANGPTL4*). Notch inhibition in HUVEC led to increased expression of *ANGPTL4* mRNA, whereas Notch1-ICD decreased it (Figure 6A). ECs isolated from the hearts or lungs of *Rbpj*$^{i\Delta EC}$ mice had increased expression levels of *Angptl4* mRNA (Figure 6C). Notch blockade in HUVEC increased ANGPTL4 protein amounts (Figure 6D). Consistently, hearts from *Rbpj*$^{i\Delta EC}$ mice contained substantially more Angptl4 protein-expressing ECs compared with controls as indicated by a stronger colocalization with lectin-GS-IB4 (Figure IV in the online-only Data Supplement), indicating that EC Notch signaling inhibits the production of the lipoprotein lipase inhibitor Angptl4.

EC Notch Signaling Induces *CD36* and *FABP4/5* to Facilitate Fatty Acid Transport

After lipolysis, fatty acid transport proteins (in particular, Fatp4) take up fatty acids into ECs. Uptake of long-chain fatty acids is supported by fatty acid translocase (CD36). Although the mRNA expression of Fatp4 and of acyl-CoA synthetases was not altered, we detected lower levels of *CD36* expression on Notch inhibition and higher CD36 mRNA levels in cells with increased Notch activity (Figure 6A). In freshly isolated cardiac and lung ECs from *Rbpj*$^{i\Delta EC}$ mice, lower CD36 mRNA expression was observed (Figure 6C), and protein regulation could be verified in primary cardiac ECs (Figure 6E). In cultured ECs, CD36 expression increased the uptake of fluorescent palmitate (Figure 6F) as reported before.[30]

Notch signaling induces the expression of fatty acid binding protein (FABP)–4, an intracellular lipid chaperone, by binding of Rbp-jκ to the FABP4 promoter.[31] We confirmed this gene regulation and found that Notch1-ICD also induces FABP5 in HUVECs. Consistently, HUVECs expressing dn Mastermind-like–1 had reduced the expression of FABP4 (Figure 6A and 6G).

EC fatty acid transport is facilitated by PPARγ, which stimulates the expression of CD36 and FABP4.[4] However, treatment of EC with the PPARγ inhibitor T0070907 did not prevent the effect of Notch1-ICD on the expression of CD36, FABP4, and ANGPTL4 (Figure 6H). Chromatin immunoprecipitation revealed that Rbp-jκ interacts with a CD36 promoter element, which contains 2 putative Rbp-jκ–binding sites (TG[G/A]GAA) (Figure 6I). Taken together, inhibition of Notch signaling led to decreased expressions of LIPG, CD36, and FABP4, whereas transcription of the lipoprotein lipase inhibitor ANGPTL4 increased, indicating that EC Notch signaling is essential for proper triacylglycerol hydrolysis and long-chain fatty acid transport.

EC-Specific Rbp-jκ Ablation Changes Cardiac Nutrient Supply, Leading to Accumulation of Monosaccharides and Their Metabolites

The heart oxidizes long-chain fatty acids to generate the majority of its energy needs.[32] An imbalance of fatty acid and glucose supply has been proposed as a potential cause of cardiac remodeling and failure.[26,27]

We observed a 2-fold reduction of activated fatty acids in heart lysates of *Rbpj*$^{i\Delta EC}$ mice (Figure 5D) and expected a compensatory increase in glucose uptake and consumption. Indeed, positron emission tomography revealed that cardiac uptake of ^{18}F-fluoro-2-deoxy-D-glucose was substantially increased in *Rbpj*$^{i\Delta EC}$ mice (Figure 7A and 7B). This increase is in a similar magnitude as observed in a different mouse model, which develops impaired cardiac contractility because of decreased endothelial fatty acid transport.[3] The elevated glucose uptake was accompanied by 3-fold higher levels of glucose-6-phosphate in hearts of *Rbpj*$^{i\Delta EC}$ mice (5–6 weeks p.i.) (Figure 7C). In addition to accumulation of glucose-6-phosphate, we detected a marked increase in glucose, maltose, sucrose, and mannose, all of which can be derived from glucose in hearts of *Rbpj*$^{i\Delta EC}$ mice, whereas plasma glucose levels were decreased compared with controls (Figure 7D and 7E). Periodic acid-Schiff staining did not show signs of glycogen accumulation in hearts 6 weeks p.i. (data not shown). However, there were higher levels of pyruvate in *Rbpj*$^{i\Delta EC}$ hearts (Figure 7F). These datasets suggest that there was a shift in nutrient supply to the heart muscle with increased glucose uptake to compensate for the impaired fatty acid transport.

Cardiac Accumulation of Glucose-6-Phosphate Is Accompanied by Sustained AKT and mTOR-S6K Signaling

It is assumed that sustained accumulation of glucose-derived metabolites and increased glycolysis rates activate mTOR-S6K signaling and other pathways leading to cell hypertrophy and subsequent heart failure.[26,33–38] Therefore, we analyzed the activity of kinases that are involved in cardiac hypertrophy in heart lysates. The phosphorylation of AKT, ERK1/2, mTOR, p70S6K, and S6 was significantly enhanced in *Rbpj*$^{i\Delta EC}$ mice 7 weeks p.i. (Figure 8A and Figure VA in the online-only Data Supplement).

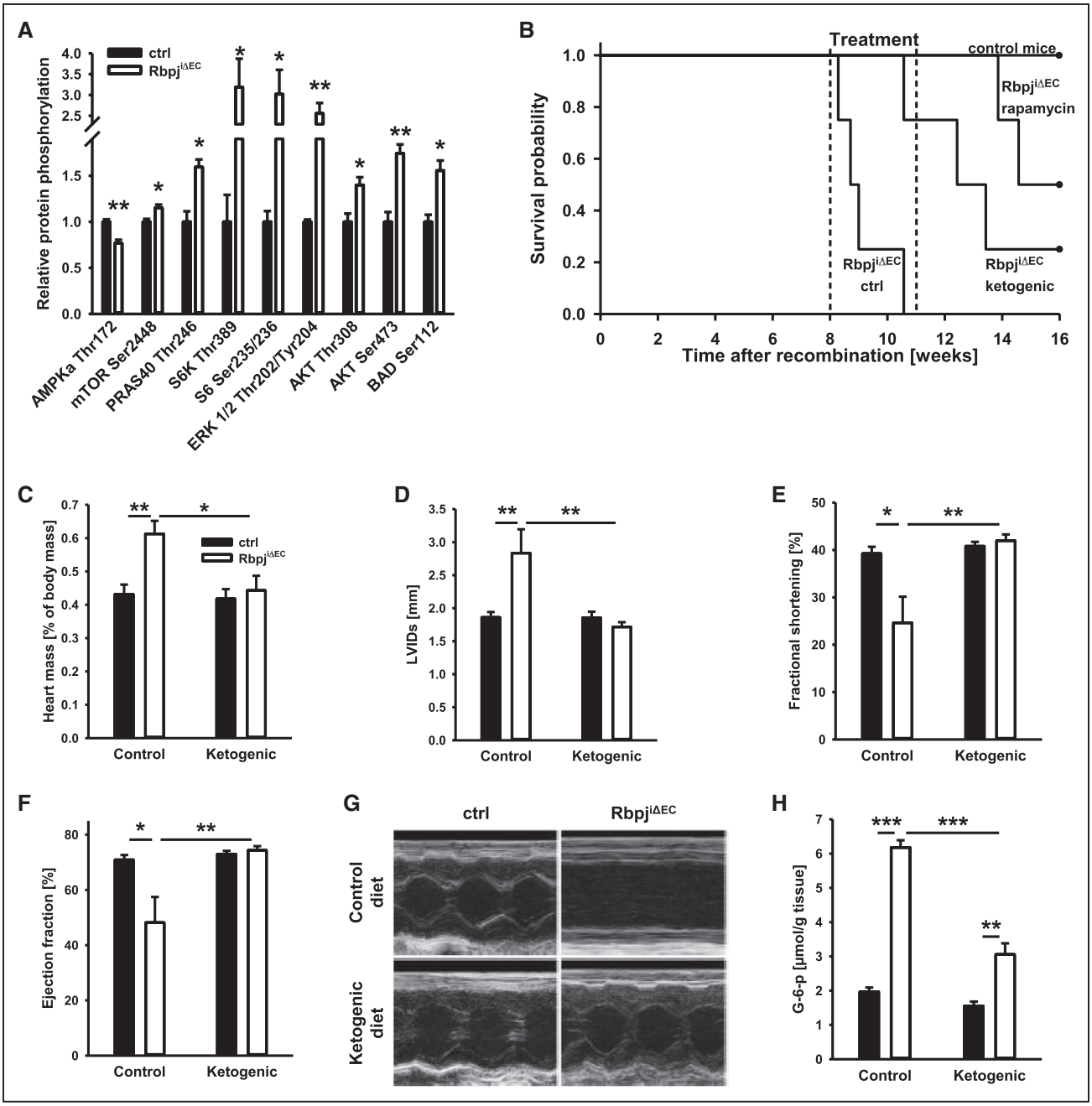

Figure 8. Reducing glucose metabolism by ketogenic diet prevents failure of *Rbpj*$^{i\Delta EC}$ hearts.
A, Phosphorylation of several kinases from the insulin, AMPK (AMP-activated protein kinase), and mTOR (mechanistic target of rapamycin) pathways in the hearts of *Rbpj*$^{i\Delta EC}$ mice (n=4 hearts). **B,** From 8 to 11 weeks after gene recombination, *Rbpj*$^{i\Delta EC}$ and control mice were treated with rapamycin and control diet, vehicle and ketogenic diet, or vehicle and control diet. Mice receiving the ketogenic diet were additionally pretreated with a high-fat diet for 2 weeks (n=4 control and 5 *Rbpj*$^{i\Delta EC}$ mice). **C,** Heart–to–body-weight ratio. **D** and **G,** *Rbpj*$^{i\Delta EC}$ and control mice were fed ketogenic and control diets, respectively, starting with gene recombination (n≥4 mice). **E** through **G,** Transthoracic echocardiography (n≥4 mice). **H,** Glucose-6-phosphate (G-6-p) levels in hearts from mice kept on control or ketogenic diet (n=4). AKT indicates protein kinase B; BAD, bcl2-associated agonist of cell death; ERK, mitogen-activated protein kinase; LVIDs, left ventricle inner diameter during systole; PRAS40, proline-rich AKT1 substrate 40kDa; S6, ribosomal protein; and S6K, ribosomal protein S6 kinase β-1. Mean and SEM or representative pictures shown. **P*<0.05; ***P*<0.01; ****P*<0.001.

To test how glucose or its metabolites act on S6K activation, freshly isolated neonatal rat cardiomyocytes were treated with 5 g/L glucose. This led to robust induction of S6K activity. 3-O-methyl-glucose alone, which is taken up by cells but is not phosphorylated and metabolized, did not activate S6K and did not prevent

glucose-induced S6K activation. However, 2-deoxyglucose, an inhibitor of glycolysis, prevented glucose-mediated induction of S6K activity (Figure VB in the online-only Data Supplement).

Interventional Therapy With Rapamycin or Feeding a Ketogenic Diet Prolongs Survival of *Rbpj*$^{i\Delta EC}$ Mice

Rbpj$^{i\Delta EC}$ mice developed severely impaired heart function around 8 to 10 weeks p.i., which was associated with increased mTOR-S6K activity. Rapamycin inhibits mTOR signaling and prevents mTOR-mediated cardiac hypertrophy and heart failure in rodent models.[37,38] We treated *Rbpj*$^{i\Delta EC}$ mice with rapamycin (2 mg/kg IP every day) 8 to 11 weeks after gene recombination. Sham-treated *Rbpj*$^{i\Delta EC}$ mice died in this period, whereas rapamycin-treated mice had a strongly increased survival rate (P=0.02) (Figure 8B).

Because rapamycin has a strong immunosuppressive effect, we also searched for alternative treatments. We propose that the impairment of heart function in *Rbpj*$^{i\Delta EC}$ mice occurs to a large extent because of a shift from long-chain fatty acid to carbohydrate supply to cardiomyocytes. Therefore, one could potentially interfere by restricting the availability of glucose to a minimum and increasing the supply of alternative substrates for mitochondrial oxidation, which do not require EC lipase activity and transport via CD36 and Fabp4/5 and which do not activate mTOR signaling. A strict ketogenic diet is ideally suited to fulfill these requirements. Amino acids from dietary protein are the source from which to generate glucose for nourishing erythrocytes and neurons, whereas fat is converted by hepatocytes into ketone bodies, a preferred energy substrate for cardiomyocytes. In addition, cardiac utilization of ketone bodies inhibits oxidation of fat and glucose.[34] It is important to note that ketone bodies are transported by monocarboxylate transporters, whose expression was not severely affected by the loss of Rbp-jκ (Figure VC in the online-only Data Supplement).

First, *Rbpj*$^{i\Delta EC}$ mice were fed a ketogenic diet (0.2% carbohydrates, 67% fat, 18% proteins per weight) in the time period 8 to 11 weeks p.i., which raised levels of total plasma ketone bodies by >5-fold (P<0.01). Compared with *Rbpj*$^{i\Delta EC}$ mice fed a control diet (67% carbohydrates, 4% fat, 19% proteins per weight), the *Rbpj*$^{i\Delta EC}$ mice fed a ketogenic diet survived significantly longer (P=0.03) (Figure 8B). Based on this finding, mice were fed a ketogenic diet starting immediately after gene recombination. Eight weeks later, echocardiography showed that *Rbpj*$^{i\Delta EC}$ mice fed a ketogenic diet had similar heart function to Cre-negative control animals, whereas *Rbpj*$^{i\Delta EC}$ mice fed a control diet suffered from severe heart failure (Figure 8C through 8G and Figure VD through VH in the online-only Data Supplement). The degree of impairment observed in the control-fed *Rbpj*$^{i\Delta EC}$ mice was less pronounced, as reported in Figure 2. The reason for this outcome is likely the slightly variable onset of the phenotype and because the night before the examination, 3 control-fed *Rbpj*$^{i\Delta EC}$ mice died (that had severely enlarged hearts). Consistent with the improvement of cardiac function, the levels of glucose-6-phosphate were lower in *Rbpj*$^{i\Delta EC}$ mice fed a ketogenic diet compared with those fed a control diet (Figure 8H).

DISCUSSION

This study has revealed critical and rate-limiting functions of EC Notch signaling in adult mice as a novel regulator of cardiac blood vessel growth and fatty acid transport across the vessel wall. Notch signaling controls numerous cell fate differentiation steps during development, tissue regeneration, and repair. Little is known about its roles for the maintenance of homeostasis in the adult organism. Recently, it was shown that elevated Notch activity promotes hepatic glucose production and reduces browning of adipose tissue, whereas genetic ablation of Rbp-jκ in hepatocytes or adipose cells as well as global Notch1 deficiency improved insulin sensitivity.[8,11,39] Because the metabolic status influences Notch signaling activity in hepatocytes as well as other cell types, including ECs,[8–12] we analyzed the roles of Notch in the adult endothelium of mice with an emphasis on metabolism. The data show that Notch signals in the endothelium are needed for proper transcriptional control of key genes (*Lipg*, *Angptl4*, *CD36*, *Fabp4/5*) for triacylglycerol hydrolysis and long-chain fatty acid transport through ECs. EC-specific targeting of Rbp-jκ led to impaired hydrolysis of triacylglycerol and decreased transport of long-chain fatty acids to heart muscle. This finding was associated with a switch from fatty acids to glucose as sources for energy production. Such a switch is also well known from several animal models of heart failure. Increased amounts of glycolysis intermediates can activate AKT and mTOR-S6K signaling. Sustained activity of these signaling pathways in cardiomyocytes induces cardiac hypertrophy, followed by heart failure.[35,36]

Second, this work demonstrates an essential role of Rbp-jκ for inhibiting blood vessel growth in the adult heart. Notch and Rbp-jκ inhibition during the embryofetal and perinatal periods leads to increased sprouting angiogenesis and defects in arteriovenous differentiation.[13,40,41] DLL4 neutralizing antibodies can induce the formation of vascular tumor-like structures on long-term treatment.[42] Here we show that blood vessel density was increased on deletion of Rbp-jκ in the heart. We hypothesize that any form of tissue growth (eg, cardiac hypertrophy) or tissue remodeling will result in aberrant and blood vessel growth in case Notch signaling is inhibited. It will be fascinating to decipher this idea in detail in future studies.

At this stage, one cannot definitely decide whether heart failure occurs solely because of impaired fatty acid transport in *Rbpj*$^{i\Delta EC}$ mice. Although perfusion studies did not show obvious defects, one can assume—based on studies in tumors[21]—that the remodeled cardiac vasculature is not fully functional. Nevertheless, several other observations strengthen the hypothesis that an altered nutrient supply to cardiomyocytes on EC-specific deletion of Rbp-jκ is important for the deterioration of heart function. We detected increased expression of *Angptl4*, a secreted noncompetitive inhibitor of lipoprotein lipase,[43] in ECs isolated from *Rbpj*$^{i\Delta EC}$ mice. Cardiac-specific overexpression of *Angptl4* causes heart failure in mice.[44] *Lipg* expression was impaired in *Rbpj*$^{i\Delta EC}$ mice. Mice deficient for this endothelial lipase are viable, but heart function is more impaired after aortic banding compared with controls.[45] Additionally, global deficiency for *Fabp4/Fabp5* causes cardiac metabolic remodeling and mild heart hypertrophy in mice, which was attributed to the lack of these proteins in cardiac endothelium.[46] The phenotype of *Rbpj*$^{i\Delta EC}$ mice is more severe, but one should notice that in these animals there is misregulation of a whole set of genes controlling or executing different steps of fatty acid hydrolysis and transport together with alterations in vascular patterning. Last, our interventional experiments with rapamycin and ketogenic diet further strengthened the importance of metabolic remodeling as an important cause of worsened heart function in *Rbpj*$^{i\Delta EC}$ mice. In summary, this work demonstrates the importance of angiocrine functions for the maintenance of cardiac homeostasis.

ARTICLE INFORMATION

Received May 30, 2017; accepted January 8, 2018.

The online-only Data Supplement is available with this article at http://circ.ahajournals.org/lookup/suppl/doi:10.1161/CIRCULATIONAHA.117.029733/-/DC1.

Authors

Markus Jabs, PhD; Adam J. Rose, PhD; Lorenz H. Lehmann, MD; Jacqueline Taylor, MSc; Iris Moll, MLS; Tjeerd P. Sijmonsma, BcS; Stefanie E. Herberich, PhD; Sven W. Sauer, PhD; Gernot Poschet, PhD; Giuseppina Federico, PhD; Carolin Mogler, MD; Eva-Maria Weis, MSc; Hellmut G. Augustin, DVM, PhD; Minhong Yan, PhD; Norbert Gretz, MD; Roland M. Schmid, MD; Ralf H. Adams, PhD; Hermann-Joseph Gröne, MD; Rüdiger Hell, PhD; Jürgen G. Okun, PhD; Johannes Backs, MD; Peter P. Nawroth, MD; Stephan Herzig, PhD; Andreas Fischer, MD

Correspondence

Andreas Fischer, MD, German Cancer Research Center, Vascular Signaling and Cancer, A270, Im Neuenheimer Feld 280, 69210 Heidelberg, Germany. E-mail a.fischer@dkfz.de

Affiliations

Division Vascular Signaling and Cancer (M.J., J.T., I.M., S.E.H., E.-M.W., A.F.), Division Vascular Oncology and Metastasis (H.G.A.), Division Cellular and Molecular Pathology (G.F., H.-J.G), German Cancer Research Center, Heidelberg. Joint Division Molecular Metabolic Control, German Cancer Research Center, Heidelberg, Center for Molecular Biology, and University Hospital Heidelberg, Germany (A.J.R., T.P.S.). Nutrient Metabolism and Signaling Lab, Department of Biochemistry and Molecular Biology, Monash Biomedicine Discovery Institute, Monash University, Clayton, Australia (A.J.R.). Department of Molecular Cardiology and Epigenetics (L.H.L., J.B.), Department of Cardiology (L.H.L.), Department of Endocrinology and Clinical Chemistry (P.P.N., A.F.), University Hospital Heidelberg, Germany. Center for Cardiovascular Research, Partner Site Heidelberg/Mannheim (L.H.L., J.B.). Department of General Pediatrics, Division of Inherited Metabolic Diseases, University Children's Hospital Heidelberg, Germany (S.W.S., J.G.O.). Center for Organismal Studies (G.P., R.H.), European Center for Angioscience (H.G.A., A.F.), Medical Research Center Mannheim (N.G.), University of Heidelberg, Germany. Institute for Pathology (C.M.), Department of Medicine II, Klinikum rechts der Isar (R.M.S.), Technical University of Munich, Germany. Department of Molecular Oncology, Genentech, South San Francisco, CA (M.Y.). Department of Tissue Morphogenesis, Max Planck Institute for Molecular Biomedicine, Faculty of Medicine, University of Münster, Germany (R.H.A.). Institute for Diabetes and Cancer (IDC), Joint Heidelberg-IDC Translational Diabetes Program, Helmholtz Center Munich, Neuherberg, Germany (S.H.).

Acknowledgments

We thank Kerstin Wöltje, Annika Zota, and Kathrin Schmidt for technical assistance. We thank the Metabolomics Core Technology Platform of the Excellence Cluster CellNetworks for support with high-performance liquid chromatography-based metabolite quantification and the small animal imaging facility at the German Cancer Research Center, especially Viktoria Eichwald, for excellent support with positron emission tomography scans and data analysis.

Sources of Funding

This work was supported by grants from the German Research Foundation (DFG FI 1569/3-1 to Dr Fischer; GRK880 to Dr Jabs, Dr Fischer, and Dr Augustin; SFB-TR23 to Dr Fischer and Dr Augustin; SFB1118 to Dr Gröne, Dr Backs, Dr Nawroth, and Dr Herzig), the Chica and Heinz Schaller Foundation (to Dr Fischer), the Dietmar Hopp Foundation (to Dr Nawroth), the European Union's Horizon 2020 Research and Innovation Program (Grant Agreement No. 692322 to Dr Fischer), the Clinician-Scientist Program of the German Cardiac Society (to Dr Lehmann), the German Center for Cardiovascular Research (to Dr Backs), and the German Ministry of Education and Research (to Dr Backs).

Disclosures

Dr Yan is a Genentech employee. The other authors report no conflicts of interest.

REFERENCES

1. Augustin HG, Koh GY. Organotypic vasculature: from descriptive heterogeneity to functional pathophysiology. *Science*. 2017;357:eaal2379. doi:10.1126/science.aal2379.
2. Ramasamy SK, Kusumbe AP, Adams RH. Regulation of tissue morphogenesis by endothelial cell-derived signals. *Trends Cell Biol*. 2015;25:148–157. doi: 10.1016/j.tcb.2014.11.007.
3. Coppiello G, Collantes M, Sirerol-Piquer MS, Vandenwijngaert S, Schoors S, Swinnen M, Vandersmissen I, Herijgers P, Topal B, van Loon J, Goffin J, Prósper F, Carmeliet P, García-Verdugo JM, Janssens S, Peñuelas I, Aranguren XL, Luttun A. Meox2/Tcf15 heterodimers program the heart capillary endothelium for cardiac fatty acid uptake. *Circulation*. 2015;131:815–826. doi: 10.1161/CIRCULATIONAHA.114.013721.
4. Kanda T, Brown JD, Orasanu G, Vogel S, Gonzalez FJ, Sartoretto J, Michel T, Plutzky J. PPARgamma in the endothelium regulates metabolic responses to high-fat diet in mice. *J Clin Invest*. 2009;119:110–124. doi: 10.1172/JCI36233.
5. Dijkstra MH, Pirinen E, Huusko J, Kivelä R, Schenkwein D, Alitalo K, Ylä-Herttuala S. Lack of cardiac and high-fat diet induced metabolic phenotypes in two independent strains of Vegf-b knockout mice. *Sci Rep*. 2014;4:6238. doi: 10.1038/srep06238.
6. Hagberg CE, Falkevall A, Wang X, Larsson E, Huusko J, Nilsson I, van Meeteren LA, Samen E, Lu L, Vanwildemeersch M, Klar J, Genove G, Pietras K, Stone-Elander S, Claesson-Welsh L, Ylä-Herttuala S, Lindahl P, Eriksson U. Vascular endothelial growth factor B controls endothelial fatty acid uptake. *Nature*. 2010;464:917–921. doi: 10.1038/nature08945.
7. Kivelä R, Bry M, Robciuc MR, Räsänen M, Taavitsainen M, Silvola JM, Saraste A, Hulmi JJ, Anisimov A, Mäyränpää MI, Lindeman JH, Eklund

L, Hellberg S, Hlushchuk R, Zhuang ZW, Simons M, Djonov V, Knuuti J, Mervaala E, Alitalo K. VEGF-B-induced vascular growth leads to metabolic reprogramming and ischemia resistance in the heart. *EMBO Mol Med*. 2014;6:307–321. doi: 10.1002/emmm.201303147.

8. Bi P, Shan T, Liu W, Yue F, Yang X, Liang XR, Wang J, Li J, Carlesso N, Liu X, Kuang S. Inhibition of Notch signaling promotes browning of white adipose tissue and ameliorates obesity. *Nat Med*. 2014;20:911–918. doi: 10.1038/nm.3615.
9. Gao F, Yao M, Shi Y, Hao J, Ren Y, Liu Q, Wang X, Duan H. Notch pathway is involved in high glucose-induced apoptosis in podocytes via Bcl-2 and p53 pathways. *J Cell Biochem*. 2013;114:1029–1038. doi: 10.1002/jcb.24442.
10. Pajvani UB, Qiang L, Kangsamaksin T, Kitajewski J, Ginsberg HN, Accili D. Inhibition of Notch uncouples Akt activation from hepatic lipid accumulation by decreasing mTorc1 stability. *Nat Med*. 2013;19:1054–1060. doi: 10.1038/nm.3259.
11. Pajvani UB, Shawber CJ, Samuel VT, Birkenfeld AL, Shulman GI, Kitajewski J, Accili D. Inhibition of Notch signaling ameliorates insulin resistance in a FoxO1-dependent manner. *Nat Med*. 2011;17:961–967. doi: 10.1038/nm.2378.
12. Briot A, Civelek M, Seki A, Hoi K, Mack JJ, Lee SD, Kim J, Hong C, Yu J, Fishbein GA, Vakili L, Fogelman AM, Fishbein MC, Lusis AJ, Tontonoz P, Navab M, Berliner JA, Iruela-Arispe ML. Endothelial NOTCH1 is suppressed by circulating lipids and antagonizes inflammation during atherosclerosis. *J Exp Med*. 2015;212:2147–2163. doi: 10.1084/jem.20150603.
13. Potente M, Gerhardt H, Carmeliet P. Basic and therapeutic aspects of angiogenesis. *Cell*. 2011;146:873–887. doi: 10.1016/j.cell.2011.08.039.
14. Chiorean EG, LoRusso P, Strother RM, Diamond JR, Younger A, Messersmith WA, Adriaens L, Liu L, Kao RJ, DiCioccio AT, Kostic A, Leek R, Harris A, Jimeno A. A phase I first-in-human study of enoticumab (REGN421), a fully human delta-like ligand 4 (Dll4) monoclonal antibody in patients with advanced solid tumors. *Clin Cancer Res*. 2015;21:2695–2703. doi: 10.1158/1078-0432.CCR-14-2797.
15. Smith DC, Eisenberg PD, Manikhas G, Chugh R, Gubens MA, Stagg RJ, Kapoun AM, Xu L, Dupont J, Sikic B. A phase I dose escalation and expansion study of the anticancer stem cell agent demcizumab (anti-DLL4) in patients with previously treated solid tumors. *Clin Cancer Res*. 2014;20:6295–6303. doi: 10.1158/1078-0432.CCR-14-1373.
16. Ramasamy SK, Kusumbe AP, Wang L, Adams RH. Endothelial Notch activity promotes angiogenesis and osteogenesis in bone. *Nature*. 2014;507:376–380. doi: 10.1038/nature13146.
17. Barber ED, Lands WE. Determination of acyl-CoA concentrations using pancreatic lipase. *Biochim Biophys Acta*. 1971;250:361–366.
18. Golovko MY, Murphy EJ. An improved method for tissue long-chain acyl-CoA extraction and analysis. *J Lipid Res*. 2004;45:1777–1782. doi: 10.1194/jlr.D400004-JLR200.
19. Lehmann LH, Rostosky JS, Buss SJ, Kreusser MM, Krebs J, Mier W, Enseleit F, Spiger K, Hardt SE, Wieland T, Haass M, Lüscher TF, Schneider MD, Parlato R, Gröne HJ, Haberkorn U, Yanagisawa M, Katus HA, Backs J. Essential role of sympathetic endothelin A receptors for adverse cardiac remodeling. *Proc Natl Acad Sci U S A*. 2014;111:13499–13504. doi: 10.1073/pnas.1409026111.
20. Furler SM, Cooney GJ, Hegarty BD, Lim-Fraser MY, Kraegen EW, Oakes ND. Local factors modulate tissue-specific NEFA utilization: assessment in rats using 3H-®-2-bromopalmitate. *Diabetes*. 2000;49:1427–1433.
21. Ridgway J, Zhang G, Wu Y, Stawicki S, Liang WC, Chanthery Y, Kowalski J, Watts RJ, Callahan C, Kasman I, Singh M, Chien M, Tan C, Hongo JA, de Sauvage F, Plowman G, Yan M. Inhibition of Dll4 signalling inhibits tumour growth by deregulating angiogenesis. *Nature*. 2006;444:1083–1087. doi: 10.1038/nature05313.
22. Hofmann JJ, Iruela-Arispe ML. Notch signaling in blood vessels: who is talking to whom about what? *Circ Res*. 2007;100:1556–1568. doi: 10.1161/01.RES.0000266408.42939.e4.
23. Wieland E, Rodriguez-Vita J, Liebler SS, Mogler C, Moll I, Herberich SE, Espinet E, Herpel E, Menuchin A, Chang-Claude J, Hoffmeister M, Gebhardt C, Brenner H, Trumpp A, Siebel CW, Hecker M, Utikal J, Sprinzak D, Fischer A. Endothelial Notch1 activity facilitates metastasis. *Cancer Cell*. 2017;31:355–367. doi: 10.1016/j.ccell.2017.01.007.
24. Szabadkai G, Duchen MR. Mitochondria: the hub of cellular Ca2+ signaling. *Physiology (Bethesda)*. 2008;23:84–94. doi: 10.1152/physiol.00046.2007.
25. Luo M, Anderson ME. Mechanisms of altered Ca^{2+} handling in heart failure. *Circ Res*. 2013;113:690–708. doi: 10.1161/CIRCRESAHA.113.301651.
26. Taegtmeyer H, Sen S, Vela D. Return to the fetal gene program: a suggested metabolic link to gene expression in the heart. *Ann N Y Acad Sci*. 2010;1188:191–198. doi: 10.1111/j.1749-6632.2009.05100.x.
27. Kundu BK, Zhong M, Sen S, Davogustto G, Keller SR, Taegtmeyer H. Remodeling of glucose metabolism precedes pressure overload-induced left ventricular hypertrophy: review of a hypothesis. *Cardiology*. 2015;130:211–220. doi: 10.1159/000369782.
28. Davies BS, Beigneux AP, Barnes RH 2nd, Tu Y, Gin P, Weinstein MM, Nobumori C, Nyrén R, Goldberg I, Olivecrona G, Bensadoun A, Young SG, Fong LG. GPIHBP1 is responsible for the entry of lipoprotein lipase into capillaries. *Cell Metab*. 2010;12:42–52. doi: 10.1016/j.cmet.2010.04.016.
29. O'Brien KD, Ferguson M, Gordon D, Deeb SS, Chait A. Lipoprotein lipase is produced by cardiac myocytes rather than interstitial cells in human myocardium. *Arterioscler Thromb*. 1994;14:1445–1451.
30. Goto K, Iso T, Hanaoka H, Yamaguchi A, Suga T, Hattori A, Irie Y, Shinagawa Y, Matsui H, Syamsunarno MR, Matsui M, Haque A, Arai M, Kunimoto F, Yokoyama T, Endo K, Gonzalez FJ, Kurabayashi M. Peroxisome proliferator-activated receptor-γ in capillary endothelia promotes fatty acid uptake by heart during long-term fasting. *J Am Heart Assoc*. 2013;2:e004861. doi: 10.1161/JAHA.112.004861.
31. Harjes U, Bridges E, McIntyre A, Fielding BA, Harris AL. Fatty acid-binding protein 4, a point of convergence for angiogenic and metabolic signaling pathways in endothelial cells. *J Biol Chem*. 2014;289:23168–23176. doi: 10.1074/jbc.M114.576512.
32. Gallagher D, Belmonte D, Deurenberg P, Wang Z, Krasnow N, Pi-Sunyer FX, Heymsfield SB. Organ-tissue mass measurement allows modeling of REE and metabolically active tissue mass. *Am J Physiol*. 1998;275(2 pt 1):E249–E258.
33. Buller CL, Heilig CW, Brosius FC III. GLUT1 enhances mTOR activity independently of TSC2 and AMPK. *Am J Physiol Renal Physiol*. 2011;301:F588–F596. doi: 10.1152/ajprenal.00472.2010.
34. Kolwicz SC Jr, Purohit S, Tian R. Cardiac metabolism and its interactions with contraction, growth, and survival of cardiomyocytes. *Circ Res*. 2013;113:603–616. doi: 10.1161/CIRCRESAHA.113.302095.
35. Sciarretta S, Volpe M, Sadoshima J. Mammalian target of rapamycin signaling in cardiac physiology and disease. *Circ Res*. 2014;114:549–564. doi: 10.1161/CIRCRESAHA.114.302022.
36. Wende AR, O'Neill BT, Bugger H, Riehle C, Tuinei J, Buchanan J, Tsushima K, Wang L, Caro P, Guo A, Sloan C, Kim BJ, Wang X, Pereira RO, McCrory MA, Nye BG, Benavides GA, Darley-Usmar VM, Shioi T, Weimer BC, Abel ED. Enhanced cardiac Akt/protein kinase B signaling contributes to pathological cardiac hypertrophy in part by impairing mitochondrial function via transcriptional repression of mitochondrion-targeted nuclear genes. *Mol Cell Biol*. 2015;35:831–846. doi:10.1128/MCB.01109-14.
37. McMullen JR, Sherwood MC, Tarnavski O, Zhang L, Dorfman AL, Shioi T, Izumo S. Inhibition of mTOR signaling with rapamycin regresses established cardiac hypertrophy induced by pressure overload. *Circulation*. 2004;109:3050–3055. doi: 10.1161/01.CIR.0000130641.08705.45.
38. Shioi T, McMullen JR, Tarnavski O, Converso K, Sherwood MC, Manning WJ, Izumo S. Rapamycin attenuates load-induced cardiac hypertrophy in mice. *Circulation*. 2003;107:1664–1670. doi: 10.1161/01.CIR.0000057979.36322.88.
39. Song NJ, Yun UJ, Yang S, Wu C, Seo CR, Gwon AR, Baik SH, Choi Y, Choi BY, Bahn G, Kim S, Kwon SM, Park JS, Baek SH, Park TJ, Yoon K, Kim BJ, Mattson MP, Lee SJ, Jo DG, Park KW. Notch1 deficiency decreases hepatic lipid accumulation by induction of fatty acid oxidation. *Sci Rep*. 2016;6:19377. doi: 10.1038/srep19377.
40. Liu Z, Turkoz A, Jackson EN, Corbo JC, Engelbach JA, Garbow JR, Piwnica-Worms DR, Kopan R. Notch1 loss of heterozygosity causes vascular tumors and lethal hemorrhage in mice. *J Clin Invest*. 2011;121:800–808. doi: 10.1172/JCI43114.
41. Nielsen CM, Cuervo H, Ding VW, Kong Y, Huang EJ, Wang RA. Deletion of Rbpj from postnatal endothelium leads to abnormal arteriovenous shunting in mice. *Development*. 2014;141:3782–3792. doi: 10.1242/dev.108951.
42. Yan M, Callahan CA, Beyer JC, Allamneni KP, Zhang G, Ridgway JB, Niessen K, Plowman GD. Chronic DLL4 blockade induces vascular neoplasms. *Nature*. 2010;463:E6–E7. doi: 10.1038/nature08751.
43. Chi X, Shetty SK, Shows HW, Hjelmaas AJ, Malcolm EK, Davies BS. Angiopoietin-like 4 modifies the interactions between lipoprotein lipase and its endothelial cell transporter GPIHBP1. *J Biol Chem*. 2015;290:11865–11877. doi: 10.1074/jbc.M114.623769.

44. Yu X, Burgess SC, Ge H, Wong KK, Nassem RH, Garry DJ, Sherry AD, Malloy CR, Berger JP, Li C. Inhibition of cardiac lipoprotein utilization by transgenic overexpression of Angptl4 in the heart. *Proc Natl Acad Sci U S A*. 2005;102:1767–1772. doi: 10.1073/pnas.0409564102.
45. Nakajima H, Ishida T, Satomi-Kobayashi S, Mori K, Hara T, Sasaki N, Yasuda T, Toh R, Tanaka H, Kawai H, Hirata K. Endothelial lipase modulates pressure overload-induced heart failure through alternative pathway for fatty acid uptake. *Hypertension*. 2013;61:1002–1007. doi: 10.1161/HYPERTENSIONAHA.111.201608.
46. Iso T, Maeda K, Hanaoka H, Suga T, Goto K, Syamsunarno MR, Hishiki T, Nagahata Y, Matsui H, Arai M, Yamaguchi A, Abumrad NA, Sano M, Suematsu M, Endo K, Hotamisligil GS, Kurabayashi M. Capillary endothelial fatty acid binding proteins 4 and 5 play a critical role in fatty acid uptake in heart and skeletal muscle. *Arterioscler Thromb Vasc Biol*. 2013;33:2549–2557. doi: 10.1161/ATVBAHA.113.301588.